Targeted disruption of GPR7, the endogenous receptor for neuropeptides B and W, leads to metabolic defects and adult-onset obesity

Makoto Ishii*, Hong Fei*†, and Jeffrey M. Friedman*‡§

*Laboratory of Molecular Genetics and ‡Howard Hughes Medical Institute, The Rockefeller University, New York, NY 10021

Contributed by Jeffrey M. Friedman, July 3, 2003

Gold-thioglucose (GTG) induces lesions in the ventromedial nucleus of the hypothalamus, resulting in hyperphagia and obesity. To identify genes involved in the hypothalamic regulation of energy homeostasis, we used a screen for genes that are dysregulated in GTG-induced obese mice. We found that GPR7, the endogenous G protein-coupled receptor for the recently identified ligands neuropeptide B and neuropeptide W, was down-regulated in hypothalamus after GTG treatment. Here we show that male *GPR7*−/− mice develop an adult-onset obese phenotype that progressively worsens with age and was greatly exacerbated when animals are fed a high-fat diet. *GPR7*−/− male mice were hyperphagic and had decreased energy expenditure and locomotor activity. Plasma levels of glucose, leptin, and insulin were also elevated in these mice. *GPR7*−/− male mice had decreased hypothalamic neuropeptide Y RNA levels and increased proopiomelanocortin RNA levels, a set of effects opposite to those evident in *ob*/*ob* mice. Furthermore, *ob*/*ob GPR7*−/− and *Ay*/*a GPR7*−/− double mutant male mice had an increased body weight compared with normal *ob*/*ob* or *Ay*/*a* male mice, suggesting that the obesity of *GPR7*−/− mice is independent of leptin and melanocortin signaling. Female mice did not show any significant weight increase or associated metabolic defects. These data suggest a potential role for GPR7 and its endogenous ligands, neuropeptide B and neuropeptide W, in regulating energy homeostasis independent of leptin and melanocortin signaling in a sexually dimorphic manner.

Maintenance of a stable body weight in mammals requires the precise balance of energy input (feeding) and energy output (energy expenditure). The hypothalamus has been identified as a main central regulator controlling energy homeostasis through a complex neuronal circuit involving classical neurotransmitters and a number of neuropeptides (1). Classical studies of animals with hypothalamic lesions have suggested that a "satiety center" in the ventromedial hypothalamic nucleus (VMH) can induce a state of negative energy balance and that a "feeding center" in the lateral hypothalamic area (LH) can induce a state of positive energy balance (1, 2). Thus, VMH lesions lead to hyperphagia and obesity, and LH lesions cause hypophagia and leanness. VMH lesions can be either electrolytic or chemical, as a single i.p. injection of gold-thioglucose (GTG) selectively ablates neurons in the VMH, causing obesity (3, 4). Evidence suggests that GTG selectively targets glucose responsive neurons in the VMH and induces neurotoxicity specifically because of the gold moiety (5, 6).

We set out to test the possibility that genes regulating energy homeostasis can be found by identifying cDNAs whose expression levels differed between GTG-treated and saline-treated control animals. Hypothalamic genes that are ablated or down-regulated after GTG treatment could possibly account for some part of the hyperphagic obese syndrome in mice with selective VMH lesions. In our study, we identified one such gene, *GPR7*, the endogenous G protein-coupled receptor for the newly identified neuropeptide ligands neuropeptide B (NPB) and neuropeptide W (NPW), which was down-regulated in GTG-treated animals.

GPR7 was originally cloned from human genomic DNA by a degenerate PCR screen using primers based on sequences from opioid receptors (7). In those prior studies, *in situ* hybridization showed abundant GPR7 expression in the arcuate and VMH nuclei and in other regions of the rodent brain (7, 8). Whereas humans and other mammals also express GPR8, a highly related G protein-coupled receptor, GPR8 is absent in rats and mice (8). Recently, several groups have identified endogenous peptide ligands NPB and NPW (alternatively called L7 and L8) for GPR7 and GPR8 by using reverse pharmacology (9–12). NPB and NPW are expressed from two different genes and together with GPR7 constitute a neuropeptide receptor pathway. Preliminary studies in WT mice and rats have revealed that NPB and NPW can increase or decrease food intake, increase locomotor activity, stimulate prolactin secretion, and promote analgesia (10, 12). However, the precise role of GPR7 signaling *in vivo* is unknown. To assess the physiological role of GPR7, we generated mice with targeted disruption of *GPR7* and studied the long-term consequences in energy homeostasis in these mice.

Methods

Animal Care and Maintenance. Unless otherwise indicated, all mice were maintained under the following conditions. Mice were weaned at 4 weeks of age and group-housed according to sex. Mice were maintained under a strict 12-h light/dark cycle (lights on 7 a.m.) in a temperature- and humidity-controlled room and fed ad libitum a standard rat diet (Diet 5001, 12% kcal fat, Lab Diet, St. Louis) and filtered water. All animal work was conducted in accordance with the guidelines of The Rockefeller University Laboratory Animal Research Center.

GTG Screen for Candidate Genes. Female CBA/J mice were obtained from The Jackson Laboratory and were acclimated for 1 week before injection. GTG (Sigma) was dissolved in 0.9% NaCl (0.2 g/ml) and was injected i.p. (2 mg/g of body weight) into 4-week-old mice. Control animals received saline injection (0.01 ml/g of body weight). Animals were then group-housed and fed ad libitum a standard rat diet. Four weeks after GTG injection, animals were weighed, and only mice weighing 20 g over the preinjection weight were used.

Subtraction Cloning of Differentially Expressed Genes After GTG Injection. Control and GTG-injected animals were killed by CO_2 asphyxiation, and hypothalami were dissected and snap-frozen in liquid N_2. Hypothalamic mRNAs were isolated (FastTrack mRNA extraction kit, Invitrogen), and cDNAs were synthesized

Abbreviations: GTG, gold-thioglucose; VMH, ventromedial hypothalamic nucleus; NPB, neuropeptide B; NPW, neuropeptide W; NPY, neuropeptide Y; POMC, proopiomelanocortin; IRES, internal ribosomal entry site; EGFP, enhanced GFP.

†Present address: Department of Biology, Illinois State University, Normal, IL 61790-4120.

§To whom correspondence should be addressed. E-mail: friedj@mail.rockefeller.edu.

www.pnas.org/cgi/doi/10.1073/pnas.1334189100

by using mRNA from control and GTG-treated hypothalamus (SuperScript, Invitrogen). cDNAs were ligated to *Eco*RI linkers at both ends, amplified using the linkers as the primers, and gel-purified. Five micrograms of the GTG-treated hypothalamic cDNAs was biotinylated with Photo-biotin (Vector Laboratories). Hybridization was carried out with 0.5 μg of unbiotinylated control cDNA at 70°C for 20 h, followed by 2 h of short incubation. After each incubation step, the double-stranded cDNA in the solution was removed by streptavidin. Hybridization was repeated three times. The end products were cloned in *Eco*RI-digested pBluescript vector. Individual clones were screened by colony lift and hybridization to the [γ-^{32}P]ATP-labeled end-product of the cDNA subtractive hybridization from both origins of hypothalamic cDNA of control or GTG-treated animals. Clones that hybridized to control subtracted cDNAs but not to GTG-treated ones were kept as positive candidates for differentially expressed cDNAs. Individual clones were verified by RNase protection or Northern blot analysis using standard methods.

Isolation and Cloning of Mouse Ortholog to Human GPR7. A mouse hypothalamic cDNA library was custom-constructed (Stratagene) and screened by using the partial sequence of one of the positive clones obtained from the validated cDNA clones. A 1-kb cDNA fragment containing a single ORF matching the sequence was isolated, and the nucleotide sequence was determined. A mouse genomic library (Stratagene) was screened by using the sequence as the probe. By restriction and sequence analysis, we determined that the gene is intronless and had sequence similarity to human GPR7.

Targeted Disruption of GPR7 and Generation of *GPR7*−/− and Double Mutant Mice. A stop codon-internal ribosomal entry site (IRES)-tau-enhanced GFP (EGFP)-thymidine kinase-neomycin cassette was inserted into a unique *Stu*I site in the coding sequence of a genomic clone of the *GPR7* gene. The 129/Ola embryonic stem cell line was transfected with linearized vector by electroporation. Transfected embryonic stem cells were screened by neomycin resistance and Southern analysis of *Bam*HI-digested genomic DNA to identify clones that had undergone successful homologous recombination. A heterozygote cell was expanded, and thymidine kinase-neomycin was excised by cre recombinase. Correctly targeted embryonic stem clones were injected into blastocytes and implanted into pseudopregnant mice. Chimeric mice were generated and bred to C57BL/6J female mice. Successful germ-line transimission and all genotyping were confirmed by tail genomic DNA Southern analysis. Northern blot was used to confirm disruption of GPR7 RNA. *GPR7*+/− male and female mice were alternatively backcrossed to C57BL/6J mice for six generations before each phenotypic analysis except for all 52-week-old mice and mice fed a high-fat diet (backcrossed four generations). C57/BL6J *ob*/+ and *Ay*/*a* mice were purchased from The Jackson Laboratory and mated to *GPR7*+/− mice to generate C57/BL6J double heterozygote mice. All double mutants were offspring of double heterozygote crosses. The *ob* gene was genotyped by PCR as described (13).

Body Weight, Food Intake, Metabolic Rate, and Locomotor Activity Measurements. Body weights were measured once a week for group-housed mice except for mice fed a high-fat diet (D12451, 45% kcal fat, Research Diets, New Brunswick, NJ), which were all single-caged. Food intake was measured in single-caged animals with an acclimation period of at least 1 week before measurement. Energy expenditure and locomotor activity was measured by using the Oxymax and OptoM3 system (Columbus Instruments, Columbus, OH). Mice were placed in the calorimeter chambers and stabilized for 1 day before measurements were recorded. Mice in the chambers had free access to both standard rat diet and water. Metabolic rate was considered as a "resting" value when the mice showed no movement as recorded by IR beam breaks. Locomotor activity was monitored every minute for each IR beam break in the three planes (*x*, *y*, and *z*) for the 12-h light and dark phases.

Plasma and Body Composition Measurements and Liver Histology. Mice were killed by CO_2 asphyxiation after a 4-h fast during the light cycle (food removed at 11 a.m., mice killed at 3 p.m.). Blood was collected by cardiac puncture with an EDTA-treated syringe needle. Plasma was obtained by centrifuging the blood and stored at −20°C until further analysis. Glucose was analyzed by the glucose oxidase method with a commercial glucometer (Bayer, Elkhart, IN). Insulin and leptin were measured by ELISA (Alpco, Windham, NH, and R & D Systems, respectively). Hypothalamus, whole brain, and a small piece of liver (≈150 mg) were removed and snap-frozen in liquid N_2 before body composition analysis of the same mice. Body composition was analyzed as described by a chloroform/methanol biochemical extraction using a Soxhelt system (14). Liver histology was performed after standard hematoxylin/eosin staining techniques in paraffin-embedded formaldehyde-fixed tissues.

Measurement of Hypothalamic Gene Expression. Hypothalamic RNA was extracted by using TRIzol reagent (Invitrogen) following the manufacturer's protocol. After RNA was isolated from individual hypothalami, contaminating DNA was removed with DNase I (DNAfree, Ambion) followed by cDNA synthesis by reverse transcription (Applied Biosystems). Quantitative real-time PCR from hypothalamic cDNA was performed by using the TaqMan system analyzed with the ABI Prism 7700 Sequence Detection System following the manufacturer's recommendations (Applied Biosystems). All expression data were normalized to cyclophilin expression levels from the same individual sample. The reported results are relative values comparing +/+ levels to −/− levels for each given gene with +/+ levels set to 1.0. Primer and probe sequences are available on request.

Statistics. All values are reported as means ± SEM. Results were analyzed by unpaired Student's *t* test for comparison of two means or ANOVA followed by analysis using Tukey's or Dunnet's posttest for comparisons of three or more means (PRISM 4.00 for Windows, GraphPad, San Diego). P values < 0.05 were considered significant.

Results

Identification of Hypothalamic Candidate Genes from GTG Screen. We used subtraction cloning to identify genes that were downregulated in the hypothalamus of obese GTG-treated female CBA/J mice relative to saline-treated control animals. Several clones with markedly reduced levels of hypothalamic RNA levels in GTG-treated versus saline controls were identified. These were verified by both RNase protection and Northern blot analysis of GTG-treated and saline-treated hypothalamic RNA (Fig. 1*A* and data not shown). Two independent clones corresponded to the mouse ortholog of human GPR7, an orphan G protein-coupled receptor (at the time).

Generation of *GPR7*−/− Mice. We disrupted the mouse *GPR7* gene by inserting a stop codon-IRES-tau-EGFP cassette into the single exon of the gene by homologous recombination (Fig. 1*B*). Genotype was determined by Southern blotting of tail genomic DNA (Fig. 1*C*). An intercross between heterozygote littermates produced WT (+/+), heterozygote (+/−), and knockout (−/−) mice in Mendelian ratios. Northern analysis and quantitative RT-PCR of hypothalamus from *GPR7*−/− mice confirmed a lack of full-length intact GPR7 RNA (Fig. 1*D* and data

PHYSIOLOGY

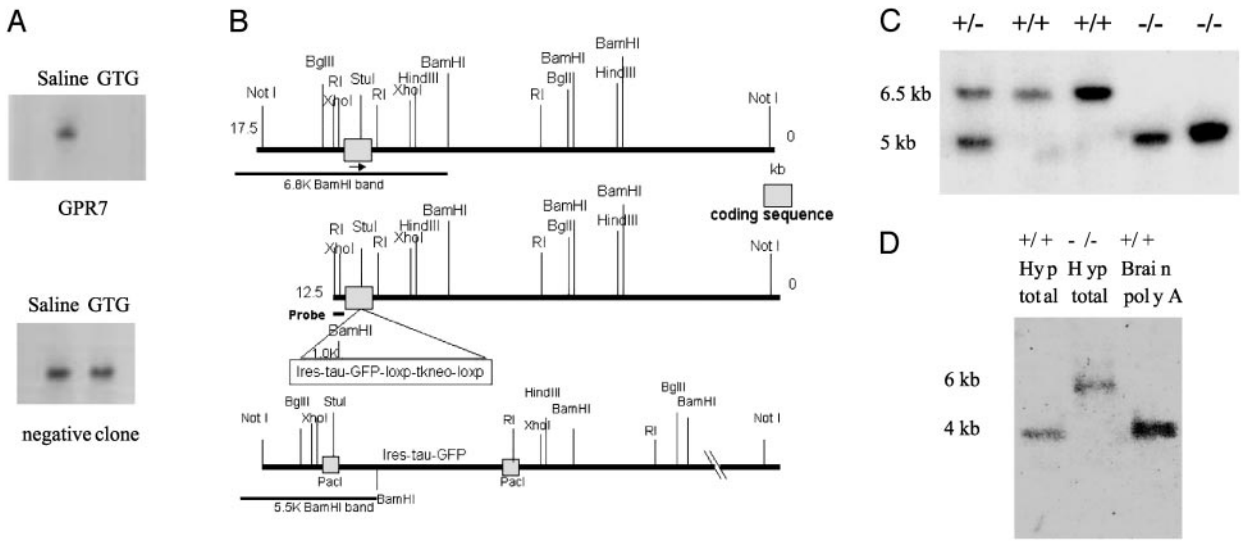

Fig. 1. GTG screen and generation of *GPR7*−/− mice. (*A*) RNase protection analysis of hypothalamic RNA from GTG-treated or saline-treated mice. (*Upper*) A GTG-regulated clone, GPR7. (*Lower*) A negative clone. (*B*) Diagram of gene-targeting strategy to disrupt the intronless *GPR7* gene with an IRES-tau-EGFP cassette. (*C*) Southern blot of tail genomic DNA from mice of heterozygote brother–sister littermate mating. WT band is ≈6.5 kb, and recombinant band is 5 kb in length. (*D*) Northern blot of hypothalamus total RNA (10 μg) from *GPR7*+/+ and *GPR7*−/− mice and poly(A)-enriched RNA from GPR7+/+ whole brain (2 μg) confirming a lack of endogenous WT GPR7 RNA transcript (4 kb) in *GPR7*−/− mice. The recombinant band is increased to 6 kb in length because of the inserted IRES-tau-EGFP cassette.

not shown). To minimize strain effects for phenotypic analysis, mice were backcrossed to C57BL/6J mice for six or more generations unless otherwise noted.

Effect of GPR7 Disruption on Body Weight and Composition. *GPR7*−/− mice were viable and fertile and showed no gross abnormalities. By 10 weeks of age, a significant increase in body weight (25.4 ± 0.4 g +/+ versus 26.9 ± 0.4 g −/−, $P < 0.05$) was evident in the male *GPR7*−/− mice. This increased weight was evident throughout adulthood and was even more pronounced by 52 weeks of age (37.1 ± 1.2 g +/+ versus 42.5 ± 1.9 g −/−, $P < 0.05$) (Fig. 2*A*). Furthermore, when the mice were fed a high-fat diet (45% kcal fat), the difference was markedly increased and also evident at an earlier age (29.4 ± 0.5 g +/+ versus 35.8 ± 1.4 g −/− at 24 weeks of age, $P < 0.05$; Fig. 2*B*). Body composition was evaluated by carcass analysis of mice at 24 and 52 weeks of age fed a low-fat diet. At 24 weeks of age, there was a trend toward higher total body lipid mass in male *GPR7*−/− mice (data not shown). At 52 weeks of age, the total body lipid mass in male *GPR7*−/− mice was double that of *GPR7*+/+ mice with *GPR7*+/− mice having an intermediate phenotype (5.83 ± 0.74 g +/+ versus 11.25 ± 1.26 g −/−, $P < 0.05$; Fig. 3*A*). At necropsy, a pale, enlarged liver was also evident in 52-week-old *GPR7*−/− male mice. Liver histology showed large vacuoles throughout the entire liver section consistent with severe hepatic steatosis (Fig. 3 *B* and *C*). Hepatic steatosis or fatty liver is a clinicopathologic syndrome that is commonly associated with obesity and the metabolic syndrome (15). In contrast, female *GPR7*−/− mice did not show any significant differences in body weight or fat mass when fed a regular or high-fat diet. (Fig. 2 *C* and *D* and data not shown).

Metabolic Defects: Food Intake, Metabolic Rate, and Locomotor Activity. We next investigated the energy intake and output in adult male mice. Food intake in these 24-week-old male *GPR7*−/− mice was consistently increased by 10% compared with *GPR7*+/+ littermates (Fig. 4*A*). Male *GPR7*−/− mice on a regular diet had decreased resting oxygen consumption (3,263 ± 116 ml/kg per h +/+ versus 2,862 ± 80 ml/kg per h −/−, $P < 0.05$; Fig. 4*A*), decreased carbon dioxide production (2,797 ± 133 ml/kg per h +/+ versus 2,346 ± 83 ml/kg per h −/−, $P < 0.05$), and decreased spontaneous locomotor activity (12-h dark cycle: 29,119 ± 2,387 beam breaks +/+ versus

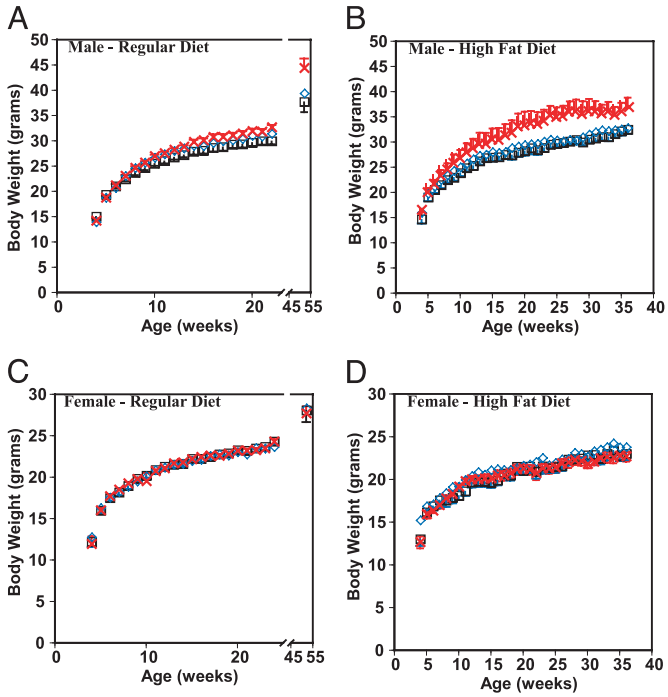

Fig. 2. Growth curves of *GPR7*−/− mice on a low-fat (*A* and *C*) and high-fat (*B* and *D*) diet. (*A* and *C*) *GPR7*+/+ (square) *GPR7*+/− (diamond), and *GPR7*−/− (cross) body weight curves on a low-fat diet for male (*A*) and female (*C*) mice ($n > 10$ for each genotype). $P < 0.05$ for *GPR7*−/− males compared with +/+ from 10 to 52 weeks of age. Not significant for female mice at any time. (*B* and *D*) *GPR7*+/+ (square), *GPR7*+/− (diamond), and *GPR7*−/− (cross) body weight curves on a high-fat (45% kcal fat) diet and single-caged from weaning for male (*B*) and female (*D*) ($n > 6$ for each genotype). $P < 0.05$ for 6–12 and 17–32 weeks of age; $P < 0.1$ for all others in male mice (not significant for female mice at any time).

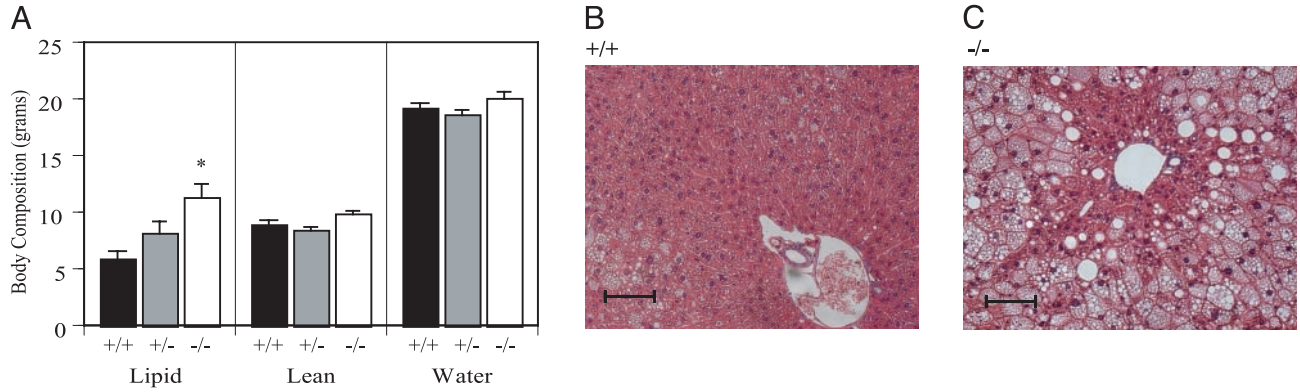

Fig. 3. Body composition analysis and liver histology of *GPR7*−/− mice fed regular chow. (*A*) Body composition for 52-week-old male mice (n = 9–17 per genotype). *, $P < 0.05$ compared with +/+ mice. (*B* and *C*) Liver histology (hematoxylin/eosin staining) from 52-week-old male *GPR7*+/+ (*B*) and *GPR7*−/− (*C*) mice. Scale bar denotes 100 μm with images at a magnification of ×200.

20,939 ± 2,312 beam breaks −/−, $P < 0.05$; Fig. 4 *C* and *D*). The combination of hyperphagia and decreased energy expenditure, possibly in part because of decreased spontaneous locomotor activity, is a likely cause of the adult-onset obesity seen in the *GPR7*−/− male mice.

Plasma Values. Analysis of plasma from 24-week-old male mice on a regular diet showed normal glucose levels but a slight increase in insulin and a trend toward higher leptin levels in *GPR7*−/− mice (Table 1). By 52 weeks of age, *GPR7*−/− mice were hyperglycemic and remained hyperinsulinemic (Table 1). The animals also became significantly hyperleptinemic with leptin levels that appear to be disproportionately high for the degree of adiposity (16). Again, no significant differences were seen in 52-week-old female mice (Table 1).

Hypothalamic Neuropeptide Levels. To explore the possible role of the adipocyte hormone leptin in the pathogenesis of the obesity in male *GPR7*−/− mice, we measured whole hypothalamic RNA levels of neuropeptide Y (NPY) and proopiomelanocortin (POMC) by using real-time quantitative RT-PCR. Leptin is secreted from adipocytes into the blood stream and acts directly on the hypothalamus, where it reduces NPY expression and activates POMC expression (1, 16, 17). In contrast to leptin-deficient *ob/ob* mice, which have increased NPY levels and decreased POMC levels, NPY levels were decreased and POMC levels were increased in *GPR7*−/− male mice (Fig. 5*A*). Levels of melanin-concentrating hormone, an orexigenic signal that is thought to be downstream of NPY and POMC, but still part of the leptin-regulated pathway, were identical in the *GPR7*+/+ and *GPR7*−/− mice (Fig. 5*A*) (18). These data suggest that the mechanism underlying obesity in *GPR7*−/− mice is different from that evident in *ob/ob* mice and that the NPY and POMC levels of these mice are more characteristic of a lean state.

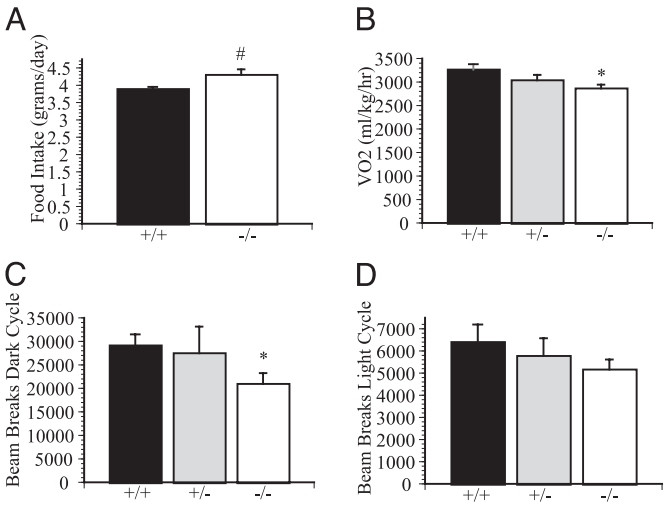

Fig. 4. Metabolic intake and expenditure of *GPR7*−/− mice. (*A*) Daily food intake of 24-week-old male mice (n = 4–6 mice in each genotype). (*B*) Resting oxygen consumption as measured in an indirect calorimeter of 24-week-old male mice (n = 7–8 in each genotype). (*C* and *D*) Total spontaneous locomotor activity of 24-week-old male mice as measured by beam breaks in the metabolic chambers for a 12-h period for dark (*C*) and light (*D*) cycle (n = 5 in each genotype). *, $P < 0.05$ compared with +/+ mice.

Body Weights of *ob/ob GPR7*−/− and *Ay/a GPR7*−/− Mice. To establish whether the effect of a GPR7 mutation was independent of the orexigenic pathways activated by leptin deficiency, double mutant *ob/ob GPR7*−/− mice were generated. The male double mutants (*ob/ob GPR7*−/−) were more obese than standard *ob/ob* mice (16 weeks of age: 55.3 ± 1.1 g *ob/ob* +/+ versus 60.0 ± 1.1 g *ob/ob* −/−, $P < 0.05$; Fig. 5*B*), whereas female double mutant mice weighed the same as normal *ob/ob* female mice at all ages (data not shown). Lethal yellow Agouti (*Ay/a*) mice, which have deficient melanocortin signaling, were also mated to generate *Ay/a GPR7*−/− mice (19). Similar to the *ob/ob GPR7*−/− animals, the male *Ay/a GPR7*−/− mice were more obese than standard *Ay/a* male mice (16 weeks of age: 38.6 ± 1.1 g *Ay/a* +/+ versus 42.3 ± 0.6 g *Ay/a* −/−, $P < 0.05$; Fig. 5*C*), whereas female *Ay/a GPR7*−/− mice again had similar body weights to female *Ay* mice (data not shown). These data strongly suggest that GPR7 affects energy homeostasis by a novel mechanism independent of the orexigenic pathways activated by defective leptin or melanocortin signaling.

Discussion

The results reported here show that GPR7 signaling plays a role in regulating energy homeostasis in mammals in a sexually dimorphic manner. We first identified *GPR7* as a candidate obesity gene because of a decrease in hypothalamic expression after GTG treatment. GPR7 mRNA expression pattern in the rodent brain is also consistent with a role in energy homeostasis. GPR7 is expressed in the arcuate and VMH of the hypothalamus, and in other regions known to regulate feeding, neuroendocrine pathways, and the autonomic nervous system (7, 8). Targeted disruption of *GPR7* in mice has confirmed that GPR7 plays a role in maintaining long-term energy homeostasis. *GPR7*−/− male mice show moderately severe, late-onset obe-

PHYSIOLOGY

Table 1. Plasma values for *GPR7*−/− mice

	Mice								
	Male, 24 weeks old			Male, 52 weeks old			Female, 52 weeks old		
Plasma	+/+	+/−	−/−	+/+	+/−	−/−	+/+	+/−	−/−
Glucose, mg/dl	208.6 ± 11.8	204.4 ± 13.6	202.25 ± 9.8	173.8 ± 8.86	200.1 ± 15.2	228.9 ± 12.6†	185.6 ± 17.6	157.9 ± 7.97	149.8 ± 7.74
Leptin, ng/ml	2.73 ± 0.61	3.40 ± 0.60	3.89 ± 0.56	11.53 ± 2.34	25.77 ± 8.33	50.10 ± 9.50†	9.04 ± 3.03	6.58 ± 1.20	5.04 ± 0.32
Insulin, ng/ml	0.76 ± 0.11	0.97 ± 0.16	1.28 ± 0.23*	3.01 ± 0.62	4.12 ± 1.15‡	7.75 ± 3.02‡	1.16 ± 0.35	1.4 ± 0.50	0.73 ± 0.11

Differences are not statistically significant unless noted. $n > 6$ for all genotypes and sexes.
*$P < 0.05$ versus +/+.
†$P < 0.005$ versus +/+.
‡$P < 0.10$ versus +/+.

sity that is a result of both hyperphagia and decreased energy expenditure with reduced locomotor activity.

The peptide ligands for GPR7 (NPB and NPW) have been recently identified by several groups using reverse pharmacology (9–12). Both peptide ligands have subnanomolar to nanomolar affinity for GPR7 and its homolog GPR8, which is absent in rodents. NPB and NPW are expressed both centrally and in the periphery (9, 12). *In situ* hybridization of NPB and NPW in the mouse brain has localized the two ligands to different neuronal populations. NPB mRNA was detected in several distinct brain regions including the hippocampus, paraventricular hypothalamic nucleus, Edinger–Westphal nucleus, motor and sensory root of the trigeminal nerve, locus coeruleus, among other areas (12). NPB had the highest expression in the Edinger–Westphal nucleus. NPW mRNA was less widespread in the mouse brain with highest mRNA levels detected in the periaqueductal gray matter, ventral tegmental area, Edinger–Westphal nucleus, and dorsal raphe nucleus (12). In periphery, NPB was highly expressed in stomach, spinal cord, and testis, whereas NPW expression was detected in stomach and lung (12). The distinct expression patterns of NPB and NPW in the brain and periphery suggest separate physiological roles for the ligands even though both act on one common receptor (GPR7) in rodents.

An intracerebroventricular (i.c.v.) bolus injection of NPB initially elicits a small and transient increase in food intake followed by a much more significant, sustained suppression of food intake during the dark cycle (12). Rats injected with NPB also have increased locomotor activity (12). The hypophagia and hyperlocomotion in rodents after an i.c.v. injection of NPB correlate well with the phenotype of *GPR7*−/− male mice. The data from the *GPR7*−/− mice further suggest that the transient increase in food intake is not likely to be biologically significant, at least over the long term. Although it is reasonable to speculate that NPB and NPW modulate food intake and energy homeostasis by binding to GPR7 in hypothalamic neurons, it is possible that the effects are mediated by nonhypothalamic neurons. Disturbances of diverse physiological systems from stress, fear, and anxiety responses to disruption of affective and emotive responses to feeding also could account for all of the phenotypes observed in the *GPR7*−/− mice. Furthermore, it is not known whether NPB and NPW exert its actions directly as a neuropeptide locally in the brain or if the peptides are also released as an endocrine hormone into the blood stream from peripheral tissues such as the stomach.

NPB and NPW have other effects, including enhancing analgesia and stimulating the release of prolactin (10, 12). The physiological relevance of these effects is unknown. The availability of *GPR7*−/− mice now provides an opportunity to distinguish nonspecific drug effects of NPB and NPW from physiological effects by comparing the ligands' effects on WT versus *GPR7*−/− mice. Thus, further studies of the effects of these peptides on body weight and other systems in normal and *GPR7*−/− mice should establish the full range of functions of the peptides *in vivo*. Because of widespread NPB and NPW mRNA expression and sequence similarity of GPR7 to opioid and somatostatin receptors, which are known to have numerous disparate physiological roles, a pleiotropic role for GPR7 signaling would not be surprising.

GPR7−/− male mice display a moderate adult-onset obese syndrome that is greatly exacerbated in animals given a high-fat diet. The moderate adult-onset obesity seen in *GPR7*−/− male mice is similar in magnitude to that seen in knockout mice for other anorexigenic hypothalamic genes. These include hormones and receptors involved in the melanocortin and cocaine-amphetamine-related peptide pathway (20, 21); bombesin receptor subtype-3, an orphan G protein-coupled receptor from

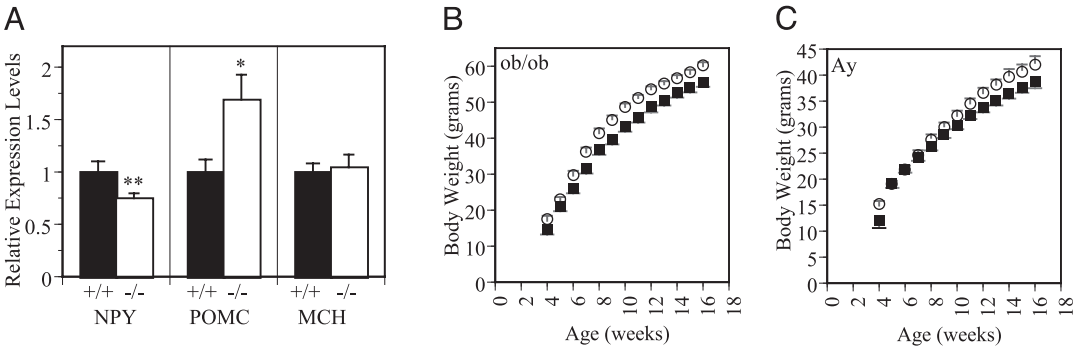

Fig. 5. GPR7 regulates energy homeostasis independent of leptin or melanocortin signaling. (*A*) Hypothalamic gene expression analysis of NPY, POMC, and melanin-concentrating hormone (MCH) using real-time quantitative RT-PCR from 24-week-old male mice. *, $P < 0.05$ compared with +/+ mice. **, $P < 0.01$ compared with +/+ mice. (*B* and *C*) Body weight curves for double *ob*/*ob GPR7*−/− mutant male (*B*) and double *Ay*/*a GPR7*−/− mutant male (*C*) mice (squares, *GPR7*+/+; circles, *GPR7*−/−; $n = 4$–15 for all genotypes). $P < 0.05$ for all male mice ages 8–16 weeks compared with WT *ob*/*ob* or *Ay*/*a* males, respectively.

the bombesin peptide receptor family (22); and other anorexigenic signals such as serotonin $5HT_{2C}$ receptor (23) and IL-6 (24). Many of these signaling molecules are components of a complex network that also includes leptin. Leptin maintains energy homeostasis by at least in part changing various RNA levels of hypothalamic neuropeptides (16). In male *GPR7*−/− mice, the hypothalamic RNA levels of NPY and POMC RNA were more characteristic of a lean rather than a leptin-deficient state. In addition, both *Ay/a GPR7*−/− and *ob/ob GPR7*−/− male mice were heavier than their respective *Ay/a* and *ob/ob GPR7*+/+ littermates. Thus, GPR7 signaling is not epistatic to leptin or melanocortins and rather appears to affect energy homeostasis by a novel mechanism independent or parallel to leptin and melanocortin signaling.

Although the physiological input(s) modulating GPR7 signaling is not known, the effects of defective GPR7 signaling are strongly sexually dimorphic. Body weight in mammals is known to be sexually dimorphic. In humans, females tend to be more obese than males, whereas in mice, males are more obese than females (25). Other animal models of hypothalamic obesity including the *NPY Y1R*−/− mice and the *NPY Y5R*−/− mice have also shown sexual dimorphism in body weight. In contrast to *GPR7*−/− male mice, *Y1R*−/− females weighed more than male *Y1R*+/+ mice, whereas similar to *GPR7*−/− male mice, *Y5R*−/− weighed more than female *Y5R*−/− (26, 27). In mice, castrating males result in decreased adiposity, whereas ovariectomizing females result in increased adiposity, indicating a strong role for sex hormones in regulating body weight (28). Although estrogens and androgens clearly modulate long-term energy homeostasis in mammals, the underlying mechanisms are unclear (29, 30). Additional investigation of the sexually dimorphic effects on body weight of *GPR7*−/− mice could lead to further elucidation of the mechanism(s) by which sex hormones regulate energy homeostasis.

In summary, these data indicate that NPB and NPW signaling via the GPR7 receptor play a biologically important role in regulating food intake, energy expenditure, and body weight. These data suggest the possibility that GPR7 agonists and possibly other components of the GPR7 signaling pathway might have therapeutic benefit for treating obesity and related metabolic conditions.

We thank the Gene Targeting Facility and DNA Sequencing Facility of The Rockefeller University for their assistance with embryonic stem cell culture work and DNA sequencing, respectively; P. Mombaerts for the IRES-tau-EGFP cassette; T. Scase and F. Quimby for assistance with the initial liver histology; L. Moy for technical assistance; P. Cohen and R. Wang for critical reading of the manuscript; and S. Korres and A. Pithart for administrative assistance. This work was supported by National Institutes of Health Medical Scientist Training Program Grant GM07739 (to M.I.), National Institutes of Health Fellowship Grant DK09604 (to H.F.), and National Institutes of Health Grant DK41096 (to J.M.F.). J.M.F. is an Investigator of the Howard Hughes Medical Institute.

1. Elmquist, J. K., Elias, C. F. & Saper, C. B. (1999) *Neuron* **22,** 221–232.
2. Hetherington, A. W. & Ranson, S. W. (1940) *Anat. Rec.* **78,** 149–172.
3. Brecher, G. & Waxler, S. M. (1949) *Proc. Soc. Exp. Biol. Med.* **70,** 498–501.
4. Marshall, N. B., Barrnett, R. J. & Mayer, J. (1955) *Proc. Soc. Exp. Biol. Med.* **90,** 240–244.
5. Mayer, J. & Marshall, N. B. (1956) *Nature* **178,** 1399–1400.
6. Debons, A. F., Krimsky, I., Maayan, M. L., Fani, K. & Jemenez, F. A. (1977) *Fed. Proc.* **36,** 143–147.
7. O'Dowd, B. F., Scheideler, M. A., Nguyen, T., Cheng, R., Rasmussen, J. S., Marchese, A., Zastawny, R., Heng, H. H. Q., Tsui, L. C., Shi, X. M., *et al*. (1995) *Genomics* **28,** 84–91.
8. Lee, D. K., Nguyen, T., Porter, C. A., Cheng, R., George, S. R. & O'Dowd, B. F. (1999) *Mol. Brain Res.* **71,** 96–103.
9. Fujii, R., Yoshida, H., Fukusumi, S., Habata, Y., Hosoya, M., Kawamata, Y., Yano, T., Hinuma, S., Kitada, C., Asami, T., *et al*. (2002) *J. Biol. Chem.* **277,** 34010–34016.
10. Shimomura, Y., Harada, M., Goto, M., Sugo, T., Matsumoto, Y., Abe, M., Watanabe, T., Asami, T., Kitada, C., Mori, M., *et al*. (2002) *J. Biol. Chem.* **277,** 35826–35832.
11. Brezillon, S., Lannoy, V., Franssen, J. D., Le Poul, E., Dupriez, V., Lucchetti, J., Detheux, M. & Parmentier, M. (2003) *J. Biol. Chem.* **278,** 776–783.
12. Tanaka, H., Yoshida, T., Miyamoto, N., Motoike, T., Kurosu, H., Shibata, K., Yamanaka, A., Williams, S. C., Richardson, J. A., Tsujino, N., *et al*. (2003) *Proc. Natl. Acad. Sci. USA* **100,** 6251–6256.
13. Erickson, J. C., Hollopeter, G. & Palmiter, R. D. (1996) *Science* **274,** 1704–1707.
14. Cohen, P., Zhao, C., Cai, X., Montez, J. M., Rohani, S. C., Feinstein, P., Mombaerts, P. & Friedman, J. M. (2001) *J. Clin. Invest.* **108,** 1113–1121.
15. Angulo, P. (2002) *N. Engl. J. Med.* **346,** 1221–1231.
16. Friedman, J. M. & Halaas, J. L. (1998) *Nature* **395,** 763–770.
17. Zhang, Y. Y., Proenca, R., Maffei, M., Barone, M., Leopold, L. & Friedman, J. M. (1994) *Nature* **372,** 425–432.
18. Qu, D., Ludwig, D. S., Gammeltoft, S., Piper, M., Pelleymounter, M. A., Cullen, M. J., Mathes, W. F., Przypek, R., Kanarek, R. & Maratos-Flier, E. (1996) *Nature* **380,** 243–247.
19. Cone, R. D. (1999) *Trends Endocrinol. Metab.* **10,** 211–216.
20. Yaswen, L., Diehl, N., Brennan, M. B. & Hochgeschwender, U. (1999) *Nat. Med.* **5,** 1066–1070.
21. Asnicar, M. A., Smith, D. P., Yang, D. D., Heiman, M. L., Fox, N., Chen, Y. F., Hsiung, H. M. & Koster, A. (2001) *Endocrinology* **142,** 4394–4400.
22. Ohki-Hamazaki, H., Watase, K., Yamamoto, K., Ogura, H., Yamano, M., Yamada, K., Maeno, H., Imaki, J., Kikuyama, S., Wada, E. & Wada, K. (1997) *Nature* **390,** 165–169.
23. Nonogaki, K., Strack, A. M., Dallman, M. F. & Tecott, L. H. (1998) *Nat. Med.* **4,** 1152–1156.
24. Wallenius, V., Wallenius, K., Ahren, B., Rudling, M., Carlsten, H., Dickson, S. L., Ohlsson, C. & Jansson, J. O. (2002) *Nat. Med.* **8,** 75–79.
25. Cortright, R. N. & Koves, T. R. (2000) *Can. J. Appl. Physiol.* **25,** 288–311.
26. Pedrazzini, T., Seydoux, J., Kunstner, P., Aubert, J. F., Grouzmann, E., Beermann, F. & Brunner, H. R. (1998) *Nat. Med.* **4,** 722–726.
27. Marsh, D. J., Hollopeter, G., Kafer, K. E. & Palmiter, R. D. (1998) *Nat. Med.* **4,** 718–721.
28. Wright, P. & Turner, C. (1973) *Physiol. Behav.* **11,** 155–159.
29. Heine, P. A., Taylor, J. A., Iwamoto, G. A., Lubahn, D. B. & Cooke, P. S. (2000) *Proc. Natl. Acad. Sci. USA* **97,** 12729–12734.
30. Jones, M. E., Thorburn, A. W., Britt, K. L., Hewitt, K. N., Wreford, N. G., Proietto, J., Oz, O. K., Leury, B. J., Robertson, K. M., Yao, S. & Simpson, E. R. (2000) *Proc. Natl. Acad. Sci. USA* **97,** 12735–12740.